Journal of Inorganic Biochemistry 153 (2015) 322–333

Contents lists available at ScienceDirect

Journal of Inorganic Biochemistry

journal homepage: www.elsevier.com/locate/jinorgbio

# Half-sandwich rhodium(III) transfer hydrogenation catalysts: Reduction of $NAD^+$ and pyruvate, and antiproliferative activity

Joan J. Soldevila-Barreda, Abraha Habtemariam, Isolda Romero-Canelón, Peter J. Sadler *

*Department of Chemistry, University of Warwick, Gibbet Hill Road, Coventry CV4 7AL, UK*

ARTICLE INFO

*Article history:*
Received 7 August 2015
Received in revised form 5 October 2015
Accepted 7 October 2015
Available online 19 October 2015

*Keywords:*
NADH
$NAD^+$
Pyruvate
Transfer-hydrogenation
Anticancer
Organo-rhodium

ABSTRACT

Organometallic complexes have the potential to behave as catalytic drugs. We investigate here Rh(III) complexes of general formula $[(Cp^x)Rh(N,N')(Cl)]$, where $N,N'$ is ethylenediamine (en), 2,2′-bipyridine (bpy), 1,10-phenanthroline (phen) or *N*-(2-aminoethyl)-4-(trifluoromethyl)benzenesulfonamide (TfEn), and $Cp^x$ is pentamethylcyclopentadienyl ($Cp^*$), 1-phenyl-2,3,4,5-tetramethylcyclopentadienyl ($Cp^{xPh}$) or 1-biphenyl-2,3,4,5-tetramethyl cyclopentadienyl ($Cp^{xPhPh}$). These complexes can reduce $NAD^+$ to NADH using formate as a hydride source under biologically-relevant conditions. The catalytic activity decreased in the order of *N*,*N*-chelated ligand bpy > phen > en with $Cp^*$ as the $\eta^5$-donor. The en complexes (**1–3**) became more active with extension to the $Cp^X$ ring, whereas the activity of the phen (**7–9**) and bpy (**4–6**) compounds decreased. $[Cp^*Rh(bpy)Cl]^+$ (**4**) showed the highest catalytic activity, with a TOF of 37.4 ± 2 $h^{-1}$. Fast hydrolysis of the chlorido complexes **1–10** was observed by $^1H$ NMR (<10 min at 310 K). The $pK_a^*$ values for the aqua adducts were determined to be ca. 8–10. Complexes **1–9** also catalysed the reduction of pyruvate to lactate using formate as the hydride donor. The efficiency of the transfer hydrogenation reactions was highly dependent on the nature of the chelating ligand and the $Cp^x$ ring. Competition reactions between $NAD^+$ and pyruvate for reduction by formate catalysed by **4** showed a preference for reduction of $NAD^+$. The antiproliferative activity of complex **3** towards A2780 human ovarian cancer cells increased by up to 50% when administered in combination with non-toxic doses of formate, suggesting that transfer hydrogenation can induce reductive stress in cancer cells.



## 1. Introduction

Transfer hydrogenation reactions for the reduction of ketones, imines or C=C double bonds have been intensively studied in recent years [1–4]. Precious metal complexes containing Ru, Rh or Ir are often effective as transfer hydrogenation catalysts, and half-sandwich organometallic complexes in particular have achieved high conversions, turnover frequencies (TOF) and enantio-selectivities [1–4]. Ruthenium(II) catalysts are often the most efficient, partly due to their slower rate of ligand exchange compared to Rh(III) or Ir(III), which, in many cases, provides higher chemo- and enantio-selectivity [1–3,5–7]. Although rhodium catalysts can be more active, this can be accompanied by a loss of chemo- and enantio-selectivity. Nevertheless, catalytic activity and enantio-selectivity depend on the choice of appropriate chiral ligands, on the substrate, the hydride donor, and on the reaction conditions [1–3,5–7].

There is current interest in metal-based complexes capable of catalysing reactions in cells [8–11]. Metallodrugs with catalytic properties can potentially be administered in smaller doses consequently leading to lower toxicity [8–11]. Transfer hydrogenation reactions have attracted much attention for the reduction of molecules inside cells [8–11]. Organo-Ru(II) and -Ir(III) complexes can catalyse hydride transfer reactions under biologically-relevant conditions (pH 7.2, 310 K, aqueous media) [12–17]. For example, $[(\eta^6\text{-arene})Ru(bipyrimidine)Cl]^+$ or $[(Cp^xIr(phenanthroline)Cl]^+$ where $Cp^X$ is pentamethylcyclopentadienyl ($Cp^*$), 1-phenyl-2,3,4,5-tetramethylcyclopentadienyl ($Cp^{xPh}$) or 1-biphenyl-2,3,4,5-tetramethylcyclopentadienyl ($Cp^{xPhPh}$) can utilise reduced nicotamide adenine dinucleotide (NADH) to transfer hydride and reduce biomolecules such as pyruvate [13,14]. The transfer of hydride to nicotinamide adenine dinucleotide ($NAD^+$) can also be achieved using formate as an hydride source, $[(\eta^6\text{-(arene)Ru(ethylendiamine)Cl}]^+$ and $[(\eta^6\text{-(arene)Ru(}N\text{-(2-aminoethyl)-sulfonamide)Cl}]^+$ where arene = *p*-cymene (*p*-cym), benzene (bn), hexamethyl benzene (hmb) or biphenyl (bip) [12,15,16].

Our recent work suggests that transfer hydrogenation catalysed by organometallic complexes can be achieved inside cells [12,13]. For example, the Ir(III) complex $[(Cp^{xphph})Ir(phenylpyrdine)py]^+$, where py is pyridine, can utilise NADH as a biological hydride donor, to generate an iridium-hydride complex. The hydrido complex is able to transfer hydride to molecular oxygen, increasing the levels of hydrogen peroxide and reactive oxygen species in cancer cells [13]. Also, the Ru(II) complex [(*p*-cym)Ru(TsEn)Cl] where TsEn is *N*-(2-aminoethyl)-

* Corresponding author.
*E-mail address:* P.J.Sadler@warwick.ac.uk (P.J. Sadler).

http://dx.doi.org/10.1016/j.jinorgbio.2015.10.008

4-toluene sulfonamide reduces the levels of $NAD^+$ in A2780 ovarian cancer cells when co-administered with sodium formate, potentiating the anti-cancer activity of the complex [12].

The aim of the present work was to synthesise a series of Rh(III) Cp* catalysts which can carry out transfer hydrogenation reactions in cells. Half-sandwich complexes of the type $[(Cp^XRh(N,N')Cl]^{n+}$, where *N,N′* = ethylenediamine (en), 2,2′-bipyridine (bpy), 2,2′-dimethylbipyridine (mbpy) and 1,10-phenanthroline (phen) were synthesised and fully characterised (Fig. 1). The activity of these Rh(III) complexes for the reduction of $NAD^+$ in the presence of formate was compared with their Ru(II) analogues [($\eta^6$-arene)Ru(en)Cl] and [($\eta^6$-arene)Ru(TsEn)Cl]. We also studied the reduction of pyruvate to lactate via hydride transfer from formate, a process carried out naturally *in vivo* by the enzyme lactate dehydrogenase and the coenzyme NADH. Finally, the antiproliferative activity of the complexes towards cancer cells in the presence of excess formate was also investigated.

## 2. Experimental

### 2.1. Materials

Rhodium(III) trichloride hydrate was purchased from Precious Metals Online (PMO Pty Ltd.) and used as received. Ethylenendiamine (en) was purchased from Sigma-Aldrich and freshly distilled prior to use. The protonated ligands 3-phenyl-1,2,4,5-tetramethyl-1,3-cyclopentadiene ($HCp^{XPh}$) and 3-biphenyl-1,2,4,5-tetramethyl-1,3-cyclopentadiene ($HCp^{xPhPh}$) were synthesised following the methods in the literature [18,19]. The Rh(III)-arene precursor dimers $[(Cp^x)RhCl_2]_2$ were prepared following literature methods [20], as was the ligand N-(2-aminoethyl)-4-(trifluoromethyl)benzenesulfonamide (TfEnH) [15]. 2,2′-Bipyridine, 4,4′-dimethyl-2,2′-dipyridine, 1,10-phenanthroline, 4-bromo-biphenyl, 4-bromo-biphenyl, 1.6 M n-butyllithium in hexane, phenyllithium in ether (1.8 mM), 2,4-pentamethylcyclopentadiene, 2,3,4,5-tetramethyl-2-cyclopentanone were obtained from Sigma-Aldrich. Magnesium sulphate, ammonium hexafluorophosphate, silver nitrate, potassium hydroxide, sodium chloride, hydrochloric acid were obtained from Fisher Scientific. Sodium formate, perchloric acid, β-nicotinamide adenine dinucleotide hydrate ($NAD^+$), β-nicotinamide adenine dinucleotide reduced disodium salt (NADH) and sodium pyruvate were purchased from Sigma-Aldrich. DMSO-$d_6$, MeOD-$d_4$, $D_2O$, $(CD_3)_2CO$-$d_6$ and $CDCl_3$ for NMR spectroscopy were purchased from Sigma-Aldrich and Cambridge Isotope Labs Inc. Non-dried solvents used in syntheses were obtained from Fisher Scientific and Prolabo.

### 2.2. NMR spectroscopy

$^1H$ NMR spectra were acquired in 5 mm NMR tubes at 298 K or 310 K on Bruker AV-400 or Bruker AV III 600 spectrometers. Data processing was carried out using XWIN-NMR version 3.6 (Bruker U.K. Ltd). $^1H$ NMR chemical shifts were internally referenced to TMS via 1,4-dioxane in $D_2O$ ($\delta = 3.75$), residual DMSO ($\delta = 2.52$ ppm) or $CHCl_3$ ($\delta = 7.26$ ppm). 1D spectra were recorded using standard pulse sequences. Typically, data were acquired with 16 transients into 32 k data points over a spectral width of 14 ppm and for the kinetic experiments, 32 transient into 32 k data points over a spectral width of 30 ppm using a relaxation delay of 2 s.

### 2.3. pH* measurements

pH* values (pH meter reading without correction for the effect of deuterium on glass electrode) were measured at ambient temperature using a minilab IQ125 pH meter equipped with a ISFET silicon chip pH sensor and referenced in KCl gel. The electrode was calibrated with Aldrich buffer solutions of pH 4, 7 and 10. pH* values were adjusted with KOH or $HClO_4$ solutions in $D_2O$.

### 2.4. Elemental analysis

Elemental analyses were performed by Warwick Analytical Service using an Exeter Analytical elemental analyzer (CE440).

### 2.5. Electrospray ionisation mass spectrometry (ESI-MS)

Positive ion electrospray mass spectra were obtained on a Bruker Daltonics Esquire 2000 ion trap mass spectrometer. All samples were prepared in methanol (100%). Data were processed using Data-Analysis version 3.3 (Bruker Daltonics).

### 2.6. Synthesis

#### 2.6.1. $[(Cp^*)RhCl_2]_2$

Hydrated rhodium(III) trichloride (500 mg, 2.12 mmol) was reacted with 2,4-pentamethylcyclopentadiene (302 mg, 2.22 mmol) dissolved in dry methanol (50 mL) and heated to reflux (343 K) under a nitrogen atmosphere for 48 h. The dark red precipitate was filtered off and washed with ether (3 × 20 mL) to give a dark red powder. The crude product was then recrystallised from methanol. Yield: 410.6 mg (62.7%). $^1H$ NMR (400 MHz, DMSO-$d_6$): $\delta_H$ 1.627 (s, 10 H).

#### 2.6.2. $[(Cp^{xPh})RhCl_2]_2$

$[(Cp^{xPh})RhCl_2]_2$ was synthesised following the same procedure described for $[(Cp^*)RhCl_2]_2$ using hydrated $Rh(III)Cl_3$ (500.7 mg, 1.05 mmol) and $HCp^{xPh}$ (532.5 mg, 2.68 mmol). The red precipitate was recrystallised from methanol. Yield: 592.7 mg (75.47%). $^1H$ NMR (400 MHz, DMSO-$d_6$): $\delta_H$ 7.67 (m, 4 H), 7.43 (m, 6 H), 1.71 (s, 4 H), 1.67 (m, 4 H).

#### 2.6.3. $[(Cp^{xPhPh})RhCl_2]_2$

$[(Cp^{xPhPh})RhCl_2]_2$ was synthesised following the procedure described for $[(Cp^*)RhCl_2]_2$ using hydrated $Rh(III)Cl_3$ (992.6 mg, 2.1 mmol) and $HCp^{xPhPh}$ (960.5 mg, 4.4 mmol). The red–orange precipitate obtained was recrystallised from methanol. Yield: 613.4 mg (33.2%). $^1H$ NMR (400 MHz, DMSO-$d_6$): $\delta_H$ 7.75 (m, 12 H), 7.49 (t, 4 H, J = 7.4 Hz), 7.40 (t, 2 H, J = 7.4 Hz), 1.73 (s, 24 H).

#### 2.6.4. General synthesis of complexes 1–9

The Rh(III) dimer was placed in a round-bottom flask to which dry dichloromethane was added. Upon addition of the corresponding ligand (2-2.5 mol. equiv.), the reaction was stirred overnight at ambient temperature, after which the solvent was removed on a rotary evaporator to afford a crude powder. The crude product was re-dissolved in methanol and filtered. Excess ammonium hexafluorophosphate was then added and the solution stored in the freezer. The resulting product was collected by filtration and recrystallised from acetone or methanol.

#### 2.6.5. $[(Cp^*)Rh(en)Cl]PF_6$ (1)

$[(Cp^*)RhCl_2]_2$ (51.3 mg, 83.0 μmol), ethylenendiamine (9.88 mg, 0.16 mmol, 11 μl). Bright yellow crystals were collected. Yield: 42.3 mg (78.3%). $^1H$ NMR (400 MHz, $CDCl_3$): $\delta_H$ 5.91 (s, 2 H), 3.05 (s, 2 H), 2.88 (s, 2 H), 2.74 (s, 2 H), 1.90 (s, 15 H). Anal: Calc for $C_{12}H_{23}ClF_6N_2PRh$ C: 27.91, H: 4.61, N: 6.21; Found C: 28.11, H: 4.81, N: 5.95. ESI-MS: Calc for $C_{12}H_{23}ClN_2O_2Rh$ $(M)^+$ 333.0 *m/z* found 333.0 *m/z*.

#### 2.6.6. $[(Cp^{xPh})Rh(en)Cl]PF_6$ (2)

$[(Cp^{xPh})RhCl_2]_2$ (50.5 mg, 68.0 μmol), ethylenendiamine (8.99 mg, 0.15 mmol, 10 μl). Recrystallisation from methanol resulted in bright yellow crystals. Yield: 31.7 mg (59.0%).$^1H$ NMR (400 MHz, $CDCl_3$): $\delta_H$ 7.49 (m, 5 H), 5.59 (s, 2 H), 3.11 (s, 2 H), 3.02 (s, 2 H), 2.76 (s, 2 H), 2.05 (s, 6 H), 1.91 (s, 6 H). Anal: Calc for $C_{17}H_{25}ClF_6N_2PRh$ C: 37.76, H: 4.66, N: 5.18; Found C: 37.02, H: 4.67, N: 5.26. ESI-MS: Calc for $C_{17}H_{25}ClN_2Rh$ $(M)^+$ 395.0 *m/z* found 395.0 *m/z*.

*2.6.7. [($Cp^{xPhPh}$)Rh(en)Cl]$PF_6$ (3)*

[($Cp^{xPhPh}$)$RhCl_2$]$_2$ (51.6 mg, 57.6 μmol), ethylenendiamine (7.11 mg, 0.12 mmol, 8 μl). Recrystallisation from methanol resulted in bright yellow crystals. Yield: 47.7 mg (54.2%) $^1$H NMR (400 MHz, $CDCl_3$): $\delta_H$ 7.69 (d, 2 H, J = 8.4 Hz), 7.60 (m, 4 H), 5.49 (t, 2 H, J = 7.5 Hz), 7.41 (t, 1 H, J = 7.5), 5.59 (s, 2 H), 3.14 (s, 2 H), 3.03 (s, 2 H), 2.79 (s, 2 H), 2.07 (s, 6 H), 1.97 (s, 6 H). Anal: Calc for $C_{23}H_{29}ClF_6N_2PRh$ C: 44.79, H: 4.74, N: 4.54; Found C: 43.98, H: 4.65, N: 4.54. ESI-MS: Calc for $C_{23}H_{29}ClN_2Rh$ $(M)^+$ 471.1 m/z, found 471.1 m/z.

*2.6.8. [($Cp^*$)Rh(bpy)Cl]$PF_6$ (4)*

[($Cp^*$)$RhCl_2$]$_2$ (100.1 mg, 162 μmol), 2,2′-bipyridine (64.7 mg, 414 μmol) Recrystallization from acetone resulted in bright orange crystals. Yield: 126.6 mg (67.9%). $^1$H NMR (400 MHz, Acetone-$d_6$): $\delta_H$ 9.14 (d, 2 H, J = 5.7 Hz), 8.67 (d, 2 H, J = 8.1 Hz), 8.38 (t, 2 H, J = 8.0 Hz),7.95 (dd, 2 H, $J_1$ = 8.0 Hz, $J_2$ = 5.7 Hz), 1.82 (s, 15 H). Anal: Calc for $C_{20}H_{23}ClF_6N_2PRh$ C: 41.8, H: 4.03, N: 4.87; Found C: 41.85, H: 3.97, N: 4.84. ESI-MS: Calc for $C_{20}H_{23}ClN_2Rh$ $(M)^+$ 430.1 *m/z* found 430.0 *m/z*.

*2.6.9. [($Cp^{XPh}$)Rh(bpy)Cl]$PF_6$ (5)*

[($Cp^{xPh}$)$RhCl_2$]$_2$ (101.3 mg, 136 μmol, 2,2′-bipyridine (56.0 mg, 359 μmol). Recrystallization from acetone resulted in bright orange crystals. Yield: 113.5 mg (65.2%).$^1$H NMR (400 MHz, Acetone-$d_6$): $\delta_H$ 8.85 (d, 2 HJ = 5.5 Hz), 8.70 (d, 2 H, J = 8.1 Hz), 8.37 (t, 2 H, J = 8.4 Hz), 7.85 (t, 2 H, J = 6.4 Hz), 7.76 (d, 2 H, J = 6.6 Hz), 7.60 (m, 3 H), 1.92 (s, 6 H), 1.85 (s, 6 H). Anal: Calc for $C_{25}H_{25}ClF_6N_2PRh$ + acetone C: 48.40, H: 4.50, N: 4.03; Found C: 49.89, H: 4.22, N: 3.93. ESI-MS: Calc for $C_{25}H_{25}ClN_2Rh$ $(M)^+$ 490.1 *m/z* found 490.0 *m/z*.

*2.6.10. [($Cp^{xPhPh}$)Rh(bpy)Cl]$PF_6$ (6)*

[($Cp^{xPhPh}$)$RhCl_2$]$_2$ (100.8 mg, 112 μmol) 2,2′-bipyridine (45.2 mg, 112 μmol). Recrystallization from acetone resulted in bright orange crystals. Yield: 87.2 mg (54.3%) $^1$H NMR (400 MHz, Acetone-$d_6$): $\delta_H$ 8.91 (d, 2 H, J = 8.2 Hz), 8.89 (d, 2 H, J = 8.4 Hz), 8.35 (t, 2 H, J = 8.0 Hz), 7.87 (m, 6 H), 7.79 (d, 2 H, J = 7.6 Hz), 7.54 (t, 2 H, J = 7.6 Hz), 7.45 (t, 1 H, J = 7.6 Hz), 1.95 (s, 6 H), 1.90 (s, 6 H). Anal: Calc for $C_{31}H_{29}ClF_6N_2PRh$ C: 52.23, H: 4.10, N: 3.93; Found C: 52.73, H: 4.31, N: 3.70. ESI-MS: Calc for $C_{31}H_{29}ClN_2Rh$ $(M)^+$ 567.1 m/z, found 567.0 m/z.

*2.6.11. [($Cp^*$)Rh(phen)Cl]$PF_6$ (7)*

[($Cp^*$)$RhCl_2$]$_2$ (100.2 mg, 162 μmol), 1,10-phenanthroline (80.78 mg, 448 μmol). Recrystallization from acetone resulted in bright orange crystals. Yield: 138.7 mg (71.4%). $^1$H NMR (400 MHz, $CDCl_3$): $\delta_H$ 9.43 (d, 2 H, J = 5.2 Hz), 8.71 (d, 2 H, 8.1 Hz), 8.29 (dd, 2 H, $J_1$ = 8.2 Hz, $J_2$ = 5.2 Hz), 8.1 (s, 2 H), 1.89 (s, 15 H). Anal: Calc for $C_{22}H_{23}ClF_6N_2PRh$ C: 44.13, H: 3.87, N: 4.68; Found C: 44.13, H: 3.79, N: 4.62. ESI-MS: Calc for $C_{22}H_{23}ClN_2Rh$ $(M)^+$ 453.1 *m/z* found 453.0 *m/z*.

*2.6.12. [($Cp^{XPh}$)Rh(phen)Cl]$PF_6$ (8)*

[($Cp^{xPh}$)$RhCl_2$]$_2$ (124.0 mg, 167 μmol), 1,10-phenanthroline (83.6 mg, 464 μmol). Recrystallization from acetone resulted in bright red crystals. Yield: 130.3 mg (59.0%).$^1$H NMR (400 MHz, $CDCl_3$): $\delta_H$ 9.08 (d, 2 H, J = 5.2 Hz), 8.69 (d, 2 H, J = 8.2 Hz), 8.12 (m, 4 H), 7.78 (d, 2 H, J = 7.6 Hz), 7.61 (m, 3 H), 2.06 (s, 6 H), 1.85 (s, 6 H). Anal: Calc for $C_{27}H_{25}ClF_6N_2PRh$ + MeOH C: 48.54, H: 4.22, N: 4.04; Found C: 47.68, H: 4.09, N: 4.17. ESI-MS: Calc for $C_{27}H_{25}ClN_2Rh$ $(M)^+$ 515.1 *m/z* found 515.0 *m/z*.

*2.6.13. [($Cp^{xPhPh}$)Rh(phen)Cl]$PF_6$ (9)*

[($Cp^{xPhPh}$)$RhCl_2$]$_2$ (100.7 mg, 112 μmol), 1,10-phenanthroline (55.8 mg, 310 μmol). Yield: 109.8 mg (66.3%) $^1$H NMR (400 MHz, $CDCl_3$): $\delta_H$ 9.11 (d, 2 H, J = 5.2 Hz), 8.69 (d, 2 H, J = 8.1 Hz), 8.13 (dd, 2 H, $J_1$ = 8.1 Hz, $J_2$ = 5.2 Hz), 8.12 (s, 2 H), 7.86 (d, 2 H, J = 8.2 Hz), 7.82 (d, 2 H, J = 8.2 Hz), 7.70 (d, 2 H J = 7.4 Hz), 7.53 (t, 2 H, J = 7.4), 7.45 (t, 1 H, J = 7.4 Hz), 2.06 (s, 6 H), 1.88 (s, 6 H). Anal: Calc for $C_{23}H_{29}ClF_6N_2PRh$ + MeOH C: 53.11, H: 4.33, N: 3.64; Found C: 54.37, H: 4.34, N: 3.49. ESI-MS: Calc for $C_{23}H_{29}ClN_2Rh$ $(M)^+$ 591.1 m/z, found 591.1 m/z.

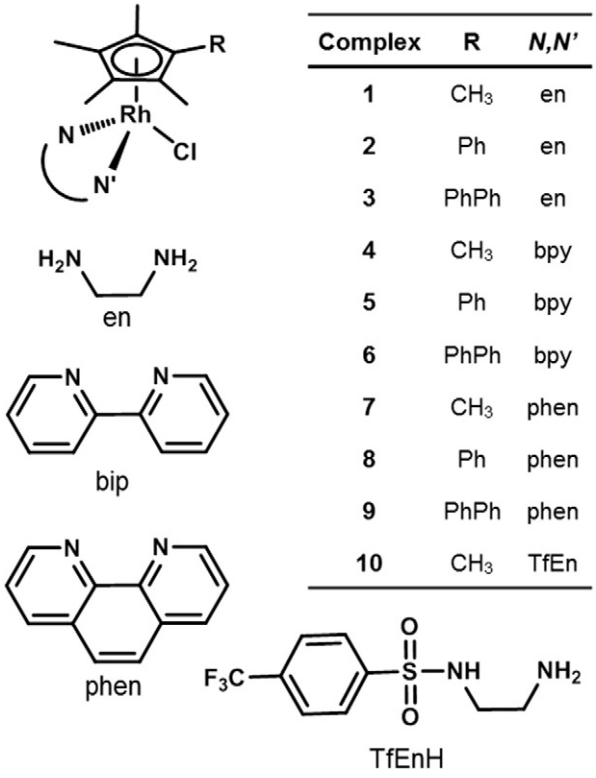


| Complex | R | N,N' |
|---|---|---|
| 1 | $CH_3$ | en |
| 2 | Ph | en |
| 3 | PhPh | en |
| 4 | $CH_3$ | bpy |
| 5 | Ph | bpy |
| 6 | PhPh | bpy |
| 7 | $CH_3$ | phen |
| 8 | Ph | phen |
| 9 | PhPh | phen |
| 10 | $CH_3$ | TfEn |

**Fig. 1.** Rh(III) complexes studied in this work, for the reduction of $NAD^+$ by transfer hydrogenation using sodium formate as a hydride source.

*2.6.14. [(Cp*)Rh(TfEn)Cl] (10)*

$[(Cp^*)RhCl_2]_2$ (49.7 mg, 80.4 μmol) and *N*-(2-aminoethyl)-4-(trifluoromethyl)benzenesulfonamide (TfEnH) (43.5 mg, 162.2 μmol) were dissolved in dichlormethane (25 mL) and triethylamine (45 μL, 320.5 μmol) was added. The reaction was then stirred under nitrogen atmosphere overnight. The solution was placed in a separating funnel and washed with brine, the organic layer separated and dried over $MgSO_4$ and filtered. The solution was concentrated in vacuo and the product recrystallised from methanol to afford an orange powder. Yield: 40.3 mg (46.4%). $^1$H NMR (400 MHz, $CDCl_3$): $\delta_H$ 8.00 (d, 2 H, J = 8.1 Hz), 7.54 (d, 2 H, J = 8.1 Hz), 3.19 (s, 2 H), 2.60 (s, 3 H), 1.71 (s, 15 H). Anal: Calc for $C_{19}H_{25}ClF_3N_2O_2RhS$ C: 42.20, H: 4.66, N: 5.18; Found C: 41.92, H: 4.36, N: 5.01. ESI-MS: Calc. for $C_{19}H_{25}ClF_3N_2O_2RhS$ $(M\text{-}Cl)^+$ 505.0 *m/z*, found 505.0 *m/z*.

### 2.7. Aqueous solution chemistry

Solutions of complexes **1–10** (1.4 mM, in 20% MeOD/80% $D_2O$) were prepared and $^1$H NMR spectra at 310 K were recorded at time 0 (<10 min) and 24 h. The samples were then incubated at 310 K.

Aqueous solutions of the chlorido complexes **1–10** (1.4 mM, in 20% MeOD/80% $D_2O$) were treated with silver nitrate (0.95 mol. equiv.) and stirred overnight at room temperature. $^1$H NMR spectra were recorded after filtration of the samples through celite to remove the silver chloride formed.

### 2.8. $pK_a$ determination for aqua species

Solutions of complexes **1–4, 7** and **10** (1.4 mM, $D_2O$) were prepared and treated with 0.95 mol equiv. of silver nitrate. The reaction mixture was then filtered through celite to obtain the corresponding aqua adducts. Changes in the chemical shifts of the methyl protons of the $Cp^x$ ligand protons on the aqua adducts with the pH* (pH meter reading) over a range from 2 to 12 were followed by $^1$H NMR spectroscopy. Solutions of KOH or $HClO_4$ in $D_2O$ were used to adjust the pH*. $^1$H-NMR spectra were recorded at 298 K on a Bruker AV III 600 spectrometer. The data were fitted to the Henderson–Hasselbalch equation using Origin 7.5.

### 2.9. Reduction of pyruvate and $NAD^+$

Complexes **1–3** and **10** were dissolved in $D_2O$ (1.4 mM, 4 mL) in a glass vial. Complexes **1–9** were prepared in MeOD/$D_2O$ (3:2 *v/v*) (1.4 mM, 4 mL) in a glass vial and treated with 0.95 mol. equiv. of silver nitrate.

Aqueous solutions of sodium formate (25 mol equiv.) and substrate (2–9 mol equiv., substrate = $NAD^+$ or pyruvate) in $D_2O$ were also prepared and incubated at 310 K. In a typical experiment, an aliquot of 200 μL of the complex, formate and substrate solutions were added to a 5 mm NMR tube. The pH* of the solution mixture was adjusted to 7.2 ± 0.2 bringing the total volume to 0.635 mL. $^1$H NMR spectra were recorded at 310 K every 162 s until the completion of the reaction.

Molar ratios of substrate and product were determined by integrating the peaks for $NAD^+$, pyruvate, lactate and 1,4-NADH. The turnover number (TON) for the reaction was calculated as follows:

$$\mathrm{TON} = \frac{I_x}{I_x + I_y}\frac{[substrate]_0}{[\mathrm{Catalyst}]}$$

where $I_n$ is the integral of the signal at n ppm. x = 6.96 (NADH) or 1.32 ppm (lactate). y = 9.33 ($NAD^+$) or 2.36 ppm (pyruvate). $[substrate]_0$ is the concentration of $NAD^+$ or pyruvate at the start of the reaction.

### 2.10. Mechanistic studies

A set of four experiments was performed to compare the characteristics of the catalytic cycle of Rh(III) complexes **1** and **10** (1.4 mM, $D_2O$) with their Ru(II) analogues.

The turnover frequencies for the reduction reaction of $NAD^+$ using complexes **1** or **10** and formate (25 mol equiv.) were determined following the procedure described above. The reaction was studied using different concentrations of $NAD^+$ (1, 2 and 5 mol equiv. for complex **10**; 5, 7.5 and 10 mol equiv. for complex **1**).

A second series of experiments using different concentrations of sodium formate (5, 10, 25, 50 and 100 mol equiv. for complex **1**; 10, 25, 50, 100 and 500 mol equiv. for complex **10**) and a constant concentration of $NAD^+$ (5 mol equiv.) was also performed.

The optimum pH range for the catalytic process was studied in a series of experiments. Each experiment was performed at a different pH* over a range from 6 to 10. The pH* of the reaction was adjusted using solutions of KOH or $HClO_4$ in $D_2O$.

Transfer hydrogenation reactions using 1,4-NADH (400 μL, 2.8 mM) as a hydride source (400 μL, 2.8 mM) in $D_2O$ by complexes **1** and **10** were studied by $^1$H NMR for a period of 10 h. The pH* of the reaction mixture was adjusted to 7.2 ± 0.2, and the experiments performed at 310 K.

### 2.11. Competition studies

Complex **1** (1.4 mM) was dissolved in $CD_3OD/D_2O$ (3:2 *v/v*,4 mL) in a glass vial. Aqueous solutions of sodium formate (100 mol equiv.), $NAD^+$ (4.5 mol equiv.) and pyruvate (4.5 mol equiv.) in $D_2O$ were also prepared and incubated at 310 K. In a typical experiment, an aliquot of 200 μL of complex, 50 μL of formate and 150 μL of pyruvate and $NAD^+$ were added to a 5 mm NMR tube. The pH* of the solution mixture was adjusted to 7.2 ± 0.2 bringing the total volume to 0.635 mL $^1$H NMR spectra were recorded at 310 K every 162 s until the completion of the reaction.

### 2.12. Antiproliferative activity and cell viability modulation assays

The antiproliferative activities of complexes **1–10** in A2780 ovarian cancer cells were determined. Briefly, 96-well plates were used to seed 5000 cells per well. The plates were pre-incubated in drug-free media at 310 K for 48 h before addition of various concentrations of the compounds. The drug exposure period was 24 h, after which, the supernatant was removed by suction and each well washed with PBS. A further 48 h was allowed for the cells to recover in drug-free medium at 310 K. The sulforhodamine B (SRB) colorimetric assay was used to determine cell viability [21]. $IC_{50}$ values, as the concentration which causes 50% growth inhibition, were determined as duplicates of triplicates in two independent sets of experiments and their standard deviations were calculated.

The data were analysed using Origin 8.5. $IC_{50}$ values were obtained from plots of the percentage survival of cells versus the logarithm of the concentration expressed in millimolar units and fitted to a sigmoidal curve. $IC_{50}$ values for cisplatin were determined in each well-plate as a validation.

Cell viability modulation assays were carried out in A2780 ovarian cancer cells. These experiments were performed as described above for $IC_{50}$ determinations with the following experimental modifications. A fixed concentration of complexes was used, 150 μM. Co-administration of the complex with three different concentrations of sodium formate (0.5, 1 and 2 mM) was studied. Both solutions (complex and sodium formate) were added to each well independently, but within 5 min of each other. Cell viability percentages were determined as duplicates of triplicates in two independent sets of experiments and their standard deviations were calculated.

Stock solutions of the Rh(III) complexes were freshly prepared for every experiment in 5% DMSO and a mixture 0.9% saline : medium (1:1 *v/v*). The stock solution was further diluted using RPMI-1640 to achieve working concentrations. The final concentration of DMSO was

between 0.5 and 0.1% *v*/*v*. Metal concentrations were determined by ICP-MS.

## 3. Results

Rh(III) complexes **1–9** were synthesised (Fig. 1) using a similar procedure. Typically, the ligand (2–2.5 mol equiv), was added to a dichloromethane solution of the rhodium dimer, $[(Cp^x)RhCl_2]_2$ and the reaction mixture stirred at ambient temperature. The details for individual reactions are described in the experimental section. Complex **10** was synthesised by reacting the dimer with the TfEnH ligand in dichloromethane, and in the presence of triethylamine (4 mol equiv) at ambient temperature overnight.

The complexes were characterised by elemental analysis, NMR spectroscopy and mass spectrometry. The x-ray crystal structures of complexes **3–6**, **8** and **9** were determined and will be reported elsewhere.

### 3.1. Aqueous solution chemistry

Aquation of complexes **1–10** (1.4 mM in 20% MeOD/ 80% $D_2O$) at 310 K was followed by $^1H$ NMR over a period of 24 h. For complexes **1–3** and **10**, only one set of peaks (aqua adducts) was observed. For complex **4–9**, two sets of peaks were observed and assigned as the chlorido and the aqua species. Peaks for aqua species were assigned by comparison of the $^1H$ spectra of **1–10** in $D_2O$ and the products of reactions between **1–10** with silver nitrate. After 24 h incubation (310 K), no apparent changes were observed by $^1H$ NMR. Compounds **6** and **9** gave rise to precipitates after 24 h and $^1H$ NMR spectra could not be recorded. The extent of hydrolysis is shown in Table 1.

Changes in the $^1H$ NMR chemical shifts of the methyl groups of cyclopentadienyl protons from the aqua adducts of complexes **1–4, 7** and **10** were followed over the pH* range from 2 to 12. The data were fitted to the Henderson–Hasselbalch equation. The $pK_a$* values for complexes **1–4, 7** and **10** are shown in Table 1 (Fig. 2).

### 3.2. Transfer hydrogenation reactions with $NAD^+$

Catalytic conversion of $NAD^+$ to NADH using complexes **1–10** and sodium formate (hydride source) was followed by $^1H$ NMR spectroscopy. In a typical experiment, 200 μL of complex (1.4 mM, $D_2O$ or MeOD/$D_2O$ 3:2 *v*/*v*), sodium formate (35 mM, $D_2O$) and $NAD^+$ (2.8–12.6 mM, $D_2O$) were mixed in a 5 mm NMR tube, final ratio 1:25:2–9, complex : sodium formate : $NAD^+$. The pH* of the reaction mixture was adjusted to 7.2 ± 0.2. $^1H$ NMR spectra at 310 K were recorded every 162 s until completion of the reaction. The turnover frequencies (TOF) for the reactions were determined as described in the experimental section (Table 2).

The turnover frequencies for complexes **1–3** in $D_2O$, increased in the order Cp *<$Cp^{xPh}$<$Cp^{xPhPh}$ (Table 2). The most active complex was $[(Cp^{xPhPh})Rh(en)Cl]^+$ (**3**), with a TOF of 24.19 $h^{-1}$. The reaction was regioselective giving 1,4-NADH exclusively. On changing the ethylendiamine (en) chelating ligand (complex **1**) to *N*-(2-aminoethyl)-4-(trifluoromethyl)benzenesulfonamide (TfEn) (complex **10**), the catalytic activity decreased (Table 2). Furthermore, a decrease in the regioselectivity of the reaction was also observed with 7.5% of 1,6-NADH being produced.

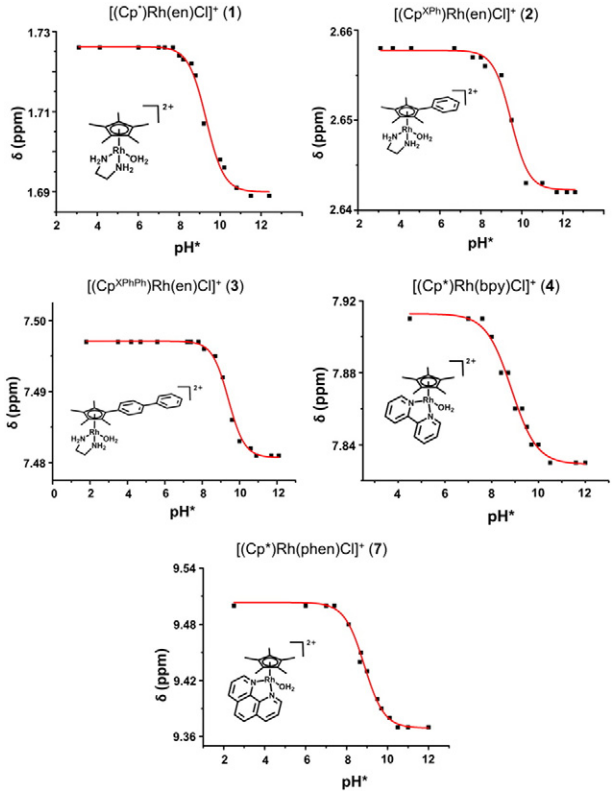


**Fig. 2.** Dependence of $^1H$ NMR chemical shifts of complexes **1–4** and **6** on pH*. The lines represent computer fits to the Henderson–Hasselbalch equation with the $pK_a$ values in Table 1.

Complex **1** was less active than complex **2** in the reduction of $NAD^+$ in 20% MeOD/80% $D_2O$, following the same trend as observed for the reaction in $D_2O$. However, the catalytic activity of complexes **1** and **2** in 20% MeOD was 2× times higher than that in $D_2O$.

Complexes **4–9** were also studied for the reduction of $NAD^+$ in 20% MeOD/80% $D_2O$. Complexes containing Cp* (**4** and **7**) were more active than those containing $Cp^{xPh}$ (**5** and **7**), which, in turn, were more active than $Cp^{xPhPh}$ complexes (**6** and **8**), (Table 2). The reactions of complexes **4–9** were largely regioselective, giving only 1 to 10% of 1,6-NADH.

**Table 1**
Hydrolysis of complexes **1–10** and $pK_a$* values for their aqua adducts.

| Complex | Hydrolysis[1] (%) | pKa*[2] |
|---|---|---|
| 1 | 100 | 9.35 ± 0.06 |
| 2 | 100 | 9.48 ± 0.06 |
| 3 | 100 | 9.35 ± 0.02 |
| 4 | 56 | 8.84 ± 0.08 |
| 5 | 38 | |
| 6 | 49 | |
| 7 | 59 | 8.86 ± 0.06 |
| 8 | 39 | |
| 9 | 48 | |
| 10 | 100 | >10 |

[1] In 20% MeOD/80% $D_2O$ (*v*/*v*) at 310 K; the reactions reached equilibrium by the time the first spectrum was recorded <10 min.
[2] In $D_2O$ at 298 K; — not determined.

**Table 2**
Turnover frequencies (TOF) for the reduction of $NAD^+$ by complexes **1–6** and **10–13**. The reactions were carried out either in $D_2O$ or 20% MeOD/80% $D_2O$ (*v*/*v*) using 6–9 mol equiv. $NAD^+$ and 25 mol equiv. formate. pH* was adjusted to 7.2 ± 0.2 and the spectra recorded at 310 K.

| Complex | $Cp^X$ | N,N′ | TOF ($h^{-1}$) $D_2O$ | TOF ($h^{-1}$) MeOD/$D_2O$ |
|---|---|---|---|---|
| 1 | Cp* | en | 7.50 ± 0.06 | 17.98 ± 0.01 |
| 2 | $Cp^{xPh}$ | en | 19.65 ± 0.01 | 35.5 ± 0.9 |
| 3 | $Cp^{xPhPh}$ | en | 24 ± 1 | – |
| 4 | Cp* | bpy | – | 37 ± 2 |
| 5 | $Cp^{xPh}$ | bpy | – | 27.7 ± 0.7 |
| 6 | $Cp^{xPhPh}$ | phen | – | 16.4 ± 0.2 |
| 7 | Cp* | phen | – | 28.0 ± 0.7 |
| 8 | $Cp^{xPh}$ | phen | – | 18.6 ± 0.5 |
| 9 | $Cp^{xPhPh}$ | phen | – | 8.2 ± 0.3 |
| 10 | Cp* | TfEn | 4.12 ± 0.01 | – |

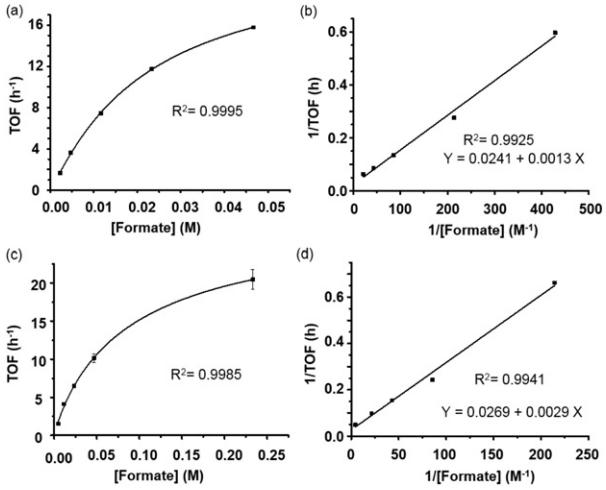


**Fig. 3.** (a) Plot of the TOF versus formate concentration (5, 10, 25, 50 or 100 mol equiv), for the reduction of $NAD^+$ catalysed by complex $[(Cp^*)Rh(en)Cl]^+$ (**1**) at pH* 7.2 and 310 K. A typical Michaelis–Menten behaviour is observed. (b) Plot of the reciprocal of the TOF against formate concentration, for catalysis by complex **1**. For Michaelis-type kinetics, $TOF^{-1} = (K_M/TOF_{max})(1/[S]) + (1/TOF_{max})$. Michaelis constant ($K_M = 54.16$ mM) and the maximum turnover frequency ($TOF_{max} = 41.49\ h^{-1}$) were determined. (c) Plot of the TOF against the formate concentration (5, 10, 25, 50 or 100 mol equiv), $TOF = TOF_{max}\,[S]/(K_M + [S])$ by complex $[(Cp^*)Rh(TfEn)Cl]^+$ (**10**) at pH* 7.2 and temperature 310 K. (d) Plot of the reciprocal of the TOF against formate concentration, for catalysis by complex **10**. For Michaelis-type kinetics, $TOF^{-1} = (K_M/TOF_{max})(1/[S]) + (1/TOF_{max})$. Michaelis constant ($K_M = 108.37$ mM) and the maximum turnover frequency ($TOF_{max} = 37.24\ h^{-1}$) were determined.

### 3.2.1. Effect of $NAD^+$ and sodium formate concentration on the catalysis rate

Transfer hydrogenation reactions using complex **1**, sodium formate and varying concentrations of $NAD^+$ were studied (ratio of 1:25:X, X = 5, 7.5 and 10 mol equiv. of $NAD^+$). The turnover frequency ($7.5\ h^{-1}$) remained the same with increasing concentrations of $NAD^+$. For complex **10,** the TOF ($4.12\ h^{-1}$) was unaffected by the concentration of $NAD^+$ (X = 1, 2 or 5 mol equiv.).

A second series of experiments on the reduction of $NAD^+$, varying the concentration of sodium formate, was performed (complex **1**, sodium formate and $NAD^+$ in the ratio 1:X:5, X = 5, 10, 25, 50 or 100 mol equiv.). A notable increase in the catalytic activity was observed with increase of the hydride source (sodium formate), (Fig. 3). From the plot of TOF vs formate concentration, typical Michaelis–Menten behaviour is observed. From the reciprocal of the TOF vs formate concentration, a maximum turnover frequency ($TOF_{max}$) of $41.49\ h^{-1}$ and a Michaelis constant ($K_M$) of 54.16 mM were calculated.

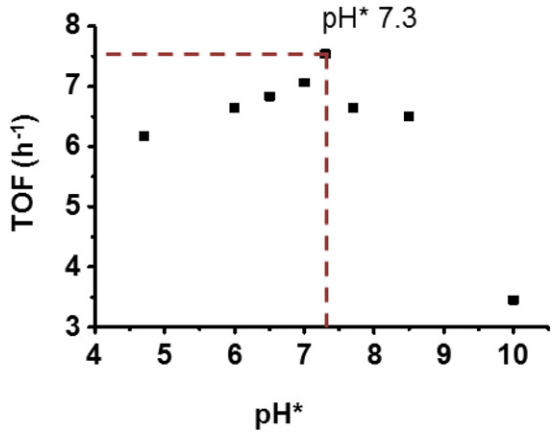


**Fig. 4.** Dependence of turnover frequency on pH* for the reduction of $NAD^+$ by complex **1** using formate as a hydride source (mol. ratio 5:1:25, respectively, 310 K in $D_2O$). Maximum turnover frequency achieved at pH* 7.3 ± 0.1.

The $TOF_{max}$ ($37.24\ h^{-1}$) and $K_M$ (108.37 mM) for complex $[(Cp^*)Rh(TfEn)Cl]$ (**10**) were also determined by performing a series of experiments with different concentrations of sodium formate (10, 25, 50, 100 or 500 mol equiv.), Fig. 3.

### 3.2.2. pH dependence

The pH* dependence of the catalytic reaction (from pH* 4 to 10) was also investigated via a series of experiments using complex **1**, sodium formate and $NAD^+$ (ratio 1:25:6, respectively) in $D_2O$. A dependence on pH* was observed. The highest TOF ($7.5\ h^{-1}$) was achieved at pH* 7.3 ± 0.1, however the turnover frequencies between pH* 6 and 8 are similar. A decrease in the catalytic activity was observed when the pH* is higher than 9 (Fig. 4).

### 3.2.3. Transfer hydrogenation reactions using NADH as a hydride donor

NADH has previously been shown to be able to act as a hydride donor [14]. As a consequence, experiments in which complexes **1–3** and **10** were reacted with NADH were performed, however, no hydride transfer from NADH was observed over a period of 10 h.

### 3.3. Transfer hydrogenation reactions with pyruvate

Lactate formation *via* hydride transfer from formate to pyruvate catalysed by complexes **1–9** was followed by $^1H$ NMR. In a typical experiment, 200 μL of complex (1.4 mM, $D_2O$ or MeOD/$D_2O$ 3:2 *v*/*v*), formate (35 mM, $D_2O$) and pyruvate (7 mM, $D_2O$) were mixed in a 5 mm NMR tube, final ratio 1:25:5, complex : formate : pyruvate. $^1H$ NMR spectra at 310 K were recorded every 162 s until completion of the reaction.

Molar ratios of pyruvate and lactate were determined by integrating the signals of pyruvate (3 H, singlet, 2.36 ppm) and of lactate (3 H, singlet, 1.32 ppm), Fig. 5. The activity of the complexes towards reduction of pyruvate to lactate is dependent on the nature of both the $Cp^X$ ring and the *N,N′* chelating ligand. Extended $Cp^{XPhPh}$ rings result in an

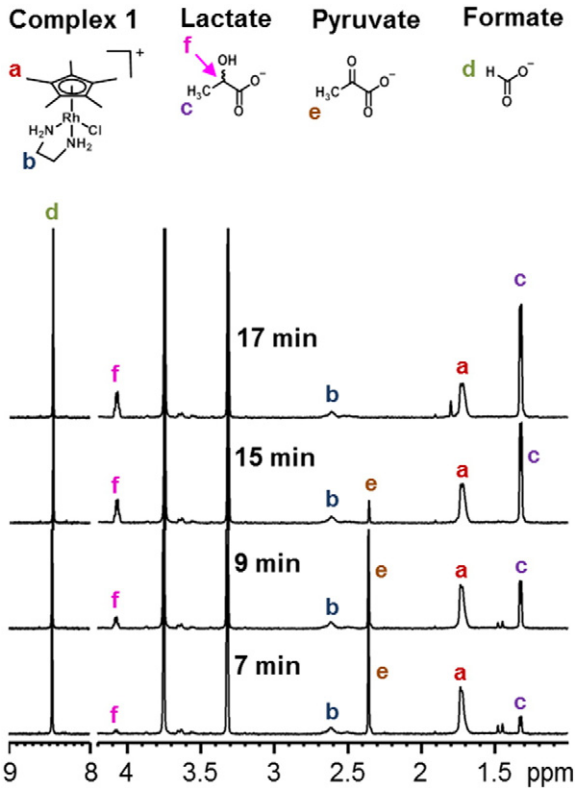


**Fig. 5.** $^1H$ NMR spectra for the reaction of complex **1**, formate and pyruvate in molar ratios of 1:25:6, respectively, in 20% MeOD/80% $D_2O$ (*v*/*v*) at 310 K and pH* 7.2 ± 0.2.

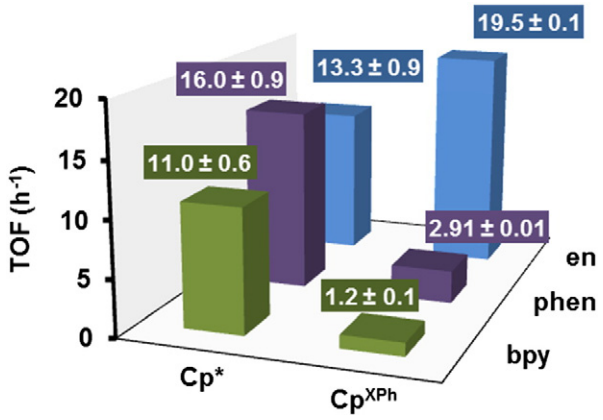


**Fig. 6.** Dependence of the turnover frequencies for the reduction of pyruvate to lactate on the $Cp^x$ ring substituent (Ph) and chelated ligand (bpy, phen or en) for complexes **1, 2, 4, 5, 7** and **8**. The reactions were carried out in 20% MeOD/80% $D_2O$ (*v*/*v*) using 6–9 mol equiv. pyruvate and 25 mol equiv. formate. The pH* was adjusted to 7.2 ± 0.2 and the NMR spectra recorded at 310 K.

increase in the catalytic activity for complexes **1** and **2**. However, there was a decrease in the TOF when the *N*,*N*′-chelated ligand is 2,2′-bipyridine (bpy) or phenanthroline (phen) (Fig. 6).

### 3.4. Competition for the reduction between $NAD^+$ and pyruvate

Transfer hydrogenation reactions with complex $[(Cp^*)Rh(bpy)Cl]^+$ (**4**), sodium formate, and both $NAD^+$ and pyruvate as hydride acceptors

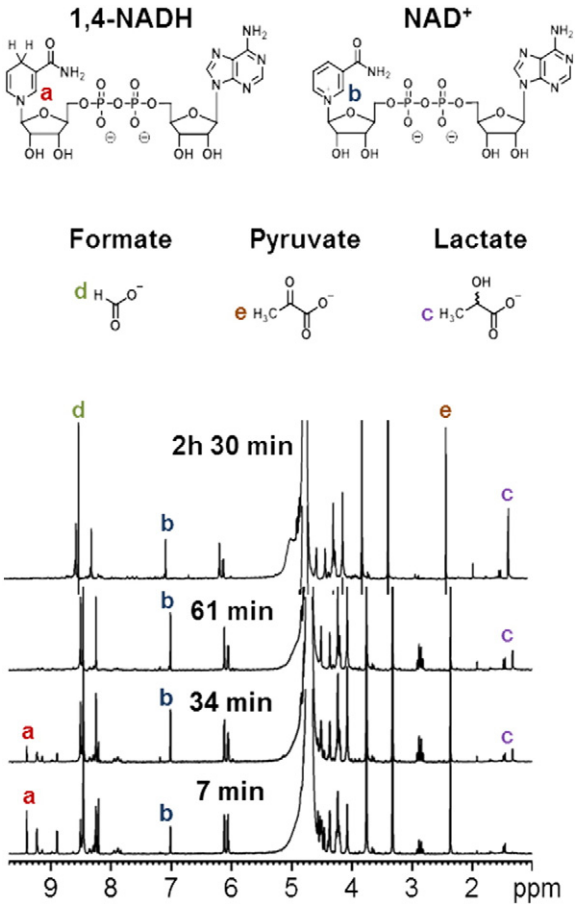


**Fig. 7.** $^1H$ NMR spectra for the reaction of complex **4**, formate and $NAD^+$ and pyruvate in molar ratios of 1:25:4.5:4.5, respectively, in 20% MeOD/80% $D_2O$ (*v*/*v*) at 310 K and pH* 7.2 ± 0.2. [1] TOF measured in $D_2O$.

were performed. For these experiments, 4.5 mol equiv. of $NAD^+$ and pyruvate were reduced using 25 mol equiv. of formate.

The reduction of both $NAD^+$ and pyruvate by complex **4** was observed, but the rate of reduction was slower for both substrates (Fig. 7). In addition, pyruvate was reduced only when the reduction of $NAD^+$ was almost complete.

### 3.5. Cancer cell growth inhibition

The $IC_{50}$ values for Rh(III) complexes **1**–**10** in A2780 human ovarian cancer cells were determined (Table 3). Complexes **1**–**3** and **10** were inactive up to the maximum concentration tested (100 μM). Complexes **4**–**9** were moderately active with $IC_{50}$ values between 14 and 65 μM.

The percentage cell survival of A2780 cells after incubation with complexes **1**–**10** and varying concentrations of sodium formate (0, 0.5, 1, 2 mM) was determined (Fig. 8). A significant increase of the antiproliferative activity of the Rh(III) complexes upon addition of formate is evident. The largest increase was observed for complex $[(Cp^{xPhPh})Rh(en)Cl]^+$ (**3**), with a decrease in cell survival of up to 50%.

## 4. Discussion

Ruthenium(II), rhodium (III) and Iridium (III) half sandwich complexes have previously been reported to catalyse the reduction of $NAD^+$ *via* transfer hydrogenation using sodium formate as a hydride source [22-24]. In the previous reports, Rh(III) complexes generally displayed higher turnover frequencies (TOF) than Ir(III), while Ru(II) complexes have the lowest catalytic activity [15,16,25–27]. However, the reported catalytic reactions were usually carried out under non-physiological conditions: high temperatures, very high concentrations of formate, pH ≠ 7.4 or with high concentrations of non-aqueous solvents [15,16,25–27].

The complexes selected for the present work have all already been studied for the reduction of $NAD^+$ under non-physiological conditions: $[(Cp^*)Rh(bpy)Cl]^+$ (**4**), developed by Steckhan and Fish [27,28], $[(Cp^*)Rh(phen)Cl]^+$ (**7**), published by Süss-Fink [26], $[(Cp^*)Rh(en)Cl]^+$ (**1**), rhodium analogue of $[(p\text{-cym})Ru(en)Cl]^+$ studied in our group [16], and $[(Cp^*)Rh(TfEn)Cl]^+$ (**10**).

Noyori-type catalysts such as $[(Cp^*)Rh(TfEn)Cl]$ (**10**) are some of the more successful catalysts for transfer hydrogenation reactions [3]. Reduction of $NAD^+$ using Noyori-type catalysts has been recently studied successfully by several groups [15,29,30].

In our previous work, we observed that the nature of arene and Cp rings can have a significant effect on the catalytic properties of half-sandwich metal complexes. For example, iridium complexes containing $Cp^x$ with extended aromatic substituents had improved catalytic activity for the regeneration of $NAD^+$ [14]. With this in mind, complexes containing $Cp^{xPh}$ and $Cp^{xPhPh}$ rings were studied in the present work.

**Table 3**
$IC_{50}$ values for complexes **1**–**10** in A2780 human ovarian cancer cells.

| Complex | $Cp^x$ | N,N′ | $IC_{50}$(μM) |
|---|---|---|---|
| 1 | $Cp^*$ | en | >100 |
| 2 | $Cp^{xPh}$ | en | >100 |
| 3 | $Cp^{xPhPh}$ | en | 100 |
| 4 | $Cp^*$ | bpy | 64 ± 1 |
| 5 | $Cp^{xPh}$ | bpy | - |
| 6 | $Cp^{xPhPh}$ | bpy | 36.07 ± 0.07 |
| 7 | $Cp^*$ | phen | 17.8 ± 0.6 |
| 8 | $Cp^{xPh}$ | phen | 57 ± 1 |
| 9 | $Cp^{xPhPh}$ | phen | 14.68 ± 0.05 |
| 10 | $Cp^*$ | TfEn | >100 |

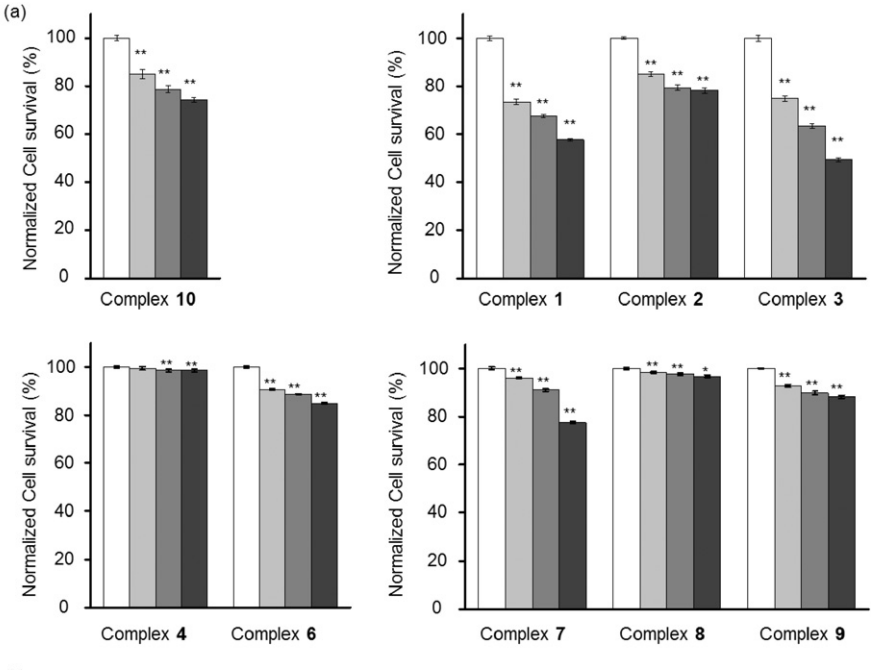


(b)

| Complex | TOF ($h^{-1}$) | Decrease in cell survival (%) | Complex | TOF ($h^{-1}$) | Decrease in cell survival (%) |
|---|---|---|---|---|---|
| 1 | 7.50 [1] / 17.98 | 42.2 | 7 | 28.0 | 22.5 |
| 2 | 19.65 [1] / 35.5 | 21.8 | 8 | 18.6 | 3.2 |
| 3 | 24 [1] | **50.6** | 9 | 8.2 | 11.7 |
| 4 | 37 | 15.1 | 10 | 4.12 [1] | 25.5 |
| 6 | 16.4 | 1.5 | | | |

[1] TOF measured in $D_2O$

**Fig. 8.** (a) Survival of A2780 human ovarian cancer cells when treated with complexes **1–4** and **6–10** (concentration = 1/3 $IC_{50}$ for **4–9**, 150 μM for **1–3** and **10**) and varying concentrations of sodium formate (key to shading of bars: 0 (white), 0.5, 1 or 2 (black) mM). $^{*}P < 0.05$, $^{**}P < 0.01$. Cell survival was normalised to the % survival of cells treated only with Rh(III) complex. (b) Table showing the % decrease in cell survival and the TOF for the reduction of $NAD^+$ (in 20% MeOD/80% $D_2O$, pH 7.2 ± 0.2, 310 K) for complexes **1–4** and **6–10**.

### 4.1. Hydrolysis and acidity of aqua adducts

Previous studies with related compounds have shown that the 16e– species or the aqua adducts of the complexes are the active catalysts in transfer hydrogenation reactions [2,31]. However, in aqueous media the presence of water and pH has been shown to play a critical role [2,31]. Aquation of the complexes **1–10** in 20% MeOD / 80% $D_2O$ (1.4 mM) was confirmed by comparing the $^1H$ NMR spectra of $D_2O$ solutions of the complexes and solutions obtained after removal of the chloride ligand by reaction with $AgNO_3$ to precipitate AgCl. Complexes **1–10** hydrolysed rapidly at 310 K, reaching equilibrium by the time the first $^1H$ NMR spectrum was recorded (<10 min). Consequently the turnover frequency for transfer hydrogenation is not affected by the use of the chlorido complex instead of the aqua adduct.

Complete conversion of the chlorido complexes **1–3** and **10** to their aqua adducts was observed. However, complexes **4–9** reached equilibrium with 30–60% formation of the aqua species (Table 1). This lower conversion would not be expected to affect the catalytic activity since the hydrolysis is fast, and the formation of hydrido species will shift the equilibria towards aqua adduct formation.

pH* titrations to determine the $pK_a$ of the aqua adducts of complexes **1–4, 7** and **10** were carried out so that the nature of the complexes at pH 7.2 (aqua or hydroxido complexes) could be determined. The formation of hydroxido adduct would be expected to hamper the catalytic reaction since hydroxido ligands bind more tightly than the aqua ligands. The $pK_a$* values of the aqua adducts determined by NMR pH* titrations, are all >8.5 (Table 1). These complexes will therefore exist largely as the aqua complexes at pH values close to 7.4.

### 4.2. Transfer hydrogenation reactions with $NAD^+$

#### 4.2.1. Comparison of Ru(II) and Rh(III)

First, we compared the catalytic activity for the reduction of $NAD^+$ by $[(Cp^*)Rh(en)Cl]^+$ (**1**) and $[(Cp^*)Rh(TfEn)Cl]$ (**13**) with the arene-Ru(II) analogues we studied previously $[(hmb)Ru(en)Cl]^+$, [(*p*-cym)Ru(TfEn)Cl] and [(bn)Ru(TfEn)Cl], (Table 4) [15,16].

The catalytic activity of the Rh(III) complexes was expected to be higher than that of their Ru(II) analogues based on the literature. [15,16,25–27] Complex **1** was up to 8.5× more active than $[(hmb)Ru(en)Cl]^+$, (Table 4). However, complex **10** had TOF values in the same range as those of the Ru analogues $[(\eta^6\text{-arene})Ru(TfEn)Cl]$ ($TOF_{p\text{-cym}} = 3.1\ h^{-1}$, $TOF_{bn} = 6.6\ h^{-1}$) [15].

The TOF of complex **10** was 2× lower than complex **1** (Table 4). This decrease in catalytic activity could be due to steric hindrance generated by the sulfonamide group. Despite the fact that half-sandwich complexes containing *N*-(2-aminoethyl)-sulfonamides are known to

**Table 4**
Comparison of the catalytic cycles of ruthenium and rhodium complexes.

| | [(p-cym)Ru(TsEn)Cl] | [(Cp*)Rh(TfEn)Cl] (10) | $[(hmb)Ru(en)Cl]^+$ | [(Cp*)Rh(en)Cl] (1) |
|---|---|---|---|---|
| Hydrolysis | Very fast[a] | Very fast | Moderate[b] | Very fast |
| % aqua adduct (24 h) | 100[a] | 100 | 32[b] | 100 |
| pK[a] | 9.71[a] | >10 | *ca.* 8[c] | 9.31 |
| TOF ($h^{-1}$) | 1.58[a] | 4.12 ± 0.01 | 0.85[d] | 7.50 ± 0.06 |
| $[NAD^+]$ dependence | No[a] | No | No[d] | No |
| $TOF_{max}$ ($h^{-1}$) | 6.4[a] | 37.2 | 1.46[d] | 41.5 |
| $K_M$ (mM) | 27.8[a] | 108.4 | 58[d] | 41.5 |
| Optimum pH* | 7.2 ± 1[a] | ND[e] | ND | 7.3 ± 0.01 |
| Reaction with 1,4 NADH | No[e] | No | ND | No |

[a] ref. [12], [b] ref. [55], [c] ref. [56], [d] ref. [16], e ND = not determined.

display very high catalytic activity for hydride transfer reactions [32,33] [3,34,35], our results are perhaps not surprising, since low catalytic activities have been previously reported with Noyori-type catalysts for the reduction of $NAD^+$ compared with other Rh(III) catalysts [30].

Next a series of ethylenediamine-Rh(III) complexes containing extended $Cp^x$ ligands was studied. A trend was observed in which the presence of a more electron-withdrawing $Cp^x$ ring gives higher catalytic activity (Table 4). Accordingly, the complex $[(Cp^{xPhPh})Rh(en)Cl]^+$ shows the highest activity followed by $[(Cp^{xPh})Rh(en)Cl]^+$ and, in turn, both are more active than $[(Cp^*)Rh(en)Cl]^+$. With **3**, an improvement in the TOF of 24× was achieved, compared with the ruthenium analogue $[(hmb)Ru(en)Cl]^+$. This increase in activity can be attributed to the effect of a less electron-rich Cp ring. The more acidic metal centre may facilitate the coordination of negatively-charged formate, which can then undergo β-elimination to generate Rh-H and $CO_2$.

In order to compare the reactivity of Cp-Rh(III) with their arene-Ru(II) analogues, a set of experiments was performed using complexes **1** and **10**: dependence of the reaction rate on the $NAD^+$ and formate concentrations, reaction with NADH, and optimum pH* of the reaction.

For reactions of $[(Cp^*)Rh(en)Cl]^+$ (**1**) and [(Cp*)Rh(TfEn)Cl] (**10**) and varying concentrations of $NAD^+$, no significant alterations in the reaction rate were observed (TOF = 7.5 and 4.1 $h^{-1}$, respectively). The unchanged turnover frequency implies that the reaction rate does not depend on the $NAD^+$ concentration. However, when the experiments were performed with increasing concentrations of the hydride source (sodium formate), the reaction rate increased, suggesting that formate is involved in the rate-determining step (Fig. 3). This behaviour is similar to that of $[(Cp^*)Rh(bpy)Cl]^+$ previously observed by Fish *et al.* [36], with the immobilised tethered Cp*Rh complex (Rh(III)-TsDPEN) where TsDPEN is (N-[(R,2R)-2-amino-1,2-diphenylethyl]-4-toluene sulfonamide) studied by Hollmann *et al.* [30] and with $[[(\eta^6\text{-arene})Ru(en)Cl]^+$ and $[[(\eta^6\text{-arene})Ru(TfEn)Cl]$ studied in our laboratory [15,16]. Plotting the turnover frequency against formate concentration shows a typical Michaelis–Menten behaviour. The maximum turnover frequency calculated from the double reciprocal of TON vs formate concentration for complex **1** is $TOF_{max}$ = 41.49 $h^{-1}$, ca. 28× higher than that of $[(hmb)Ru(en)Cl]^+$ ($TOF_{max}$ = 1.46 $h^{-1}$) [16].

The $TOF_{max}$ for complex **10** was 37.2 $h^{-1}$, only ca. 5× higher than that of [(*p*-cym)Ru(TsEn)Cl] ($TOF_{max}$ = 6.9 $h^{-1}$) [15]. At high concentrations of hydride (Sodium formate), the complexes containing TfEn ligands are 5× times more active than their ruthenium analogues. However, complex [(Cp*)Rh(TsEn)Cl] (**10**) is still less active than the ethylenediamine complex $[(Cp^*)Rh(en)Cl]^+$ (**1**).

The Michaelis constant for complex **10** ($K_M$ = 108.4 mM) indicates a weaker affinity for formate compared to complexes $[(Cp^*)Rh(en)Cl]^+$ ($K_M$ = 41.5 mM), $[(hmb)Ru(en)Cl]^+$ ($K_M$ = 58 mM), [16] and [(*p*-cym)Ru(TsEn)Cl] (42.1 mM) [15]. Compared with $[(Cp^*)Rh(bpy)H_2O]^{2+}$ ($K_M$ 140 mM) [36], complex **10** shows stronger affinity for formate. This implies that the low catalytic activity when using 25 mol equiv. of formate is due to reduced affinity for formate, but the catalytic activity increases markedly in formate-saturated solutions.

Some iridium and ruthenium complexes such as ($[Cp^*Ir(phen)Cl]^+$, ($[Cp^*Ir(phenylpyridine)Cl]$ and$[(p\text{-cym})Ru(bipyrimidine)Cl]$) have been shown to oxidise NADH through transfer hydrogenation [13,14, 17,37]. In such processes, the NADH acts as a natural hydride donor, and the metal catalyses hydride transfer from NADH to other substrates such as quinones, pyruvate or oxygen [13,14,37]. In this study, we investigated the possibility of oxidising NADH using the rhodium(III) complexes **1** and **10**. No oxidation of NADH occurred after 12 h at 310 K and pH 7.2 ± 0.2. In contrast to the above-mentioned compounds, the lack of reactivity with NADH is similar to the ruthenium complex [(*p*-cym)Ru(TfEn)Cl]. These experiments emphasise the critical influence of the ligands in half-sandwich complexes on the reactivity of the complex.

The last experiment performed was to determine the optimum pH* for the reduction of $NAD^+$. In line with our aim of applying the catalytic reduction of $NAD^+$ in biological systems, we worked at pH 7.2. However, it is interesting to note the effect of pH on the reaction rate. Surprisingly, the maximum activity for complex **1** was observed at pH* 7.3 (Fig. 3) which is close to physiological pH. Furthermore, slight variations were observed over the pH range 5 to 9. At pH* > 9, the concentration of $OH^-$ inhibits the reaction due to the formation of the more inert Rh(III) hydroxido adduct. This effect of pH was also observed for the ruthenium systems [2,15].

#### *4.2.2. Reduction of $NAD^+$*

In order to select the best catalyst candidate to work with, 3 well-known half-sandwich Rh(III) compounds were studied for their catalytic activity towards the reduction of $NAD^+$. We also studied the effect of extended phenylation of $Cp^X$ rings on their TOF. These reactions were performed in 20% MeOD and 80% $D_2O$ to aid solubility.

As we observed previously, there is an increase on the TOF for ethylendiamine-containing-complexes when using extended rings. Interestingly, there is a 2-fold increase in the TOF due to the effect of 20% MeOD. This effect was observed previously for the ruthenium(II) complexes [(arene)Ru(TfEn)Cl]] [15].

The TOF of complexes **4–9** for the reduction of $NAD^+$ decreases when using $Cp^{xPh}$ or $Cp^{xPhPh}$ as ligands (Table 2). Those results are surprising, since the trend is opposite to that for complexes **1–3**. These results may be attributable to steric factors due to the extended Cp ring and the size of the chelating ligand (bipyridine and phenanthroline compared to ethylenediamine).

The catalytic activity for the reduction of $NAD^+$ is also dependent on the *N,N′* chelating ligand. For complexes containing Cp*, the turnover frequencies increase in the order en < phen < bpy, whereas for complexes containing $Cp^{XPh}$ or $Cp^{XPhPh}$, the TOFs increase in the order phen < bpy < en (Table 2). Higher activity (TOF = 37.4 ± 2 $h^{-1}$) was obtained with $[Cp^*Rh(bpy)Cl]^+$ (**4**). However, the catalytic activity for the

reduction of $NAD^+$ ethylendiamine complex $[(Cp^{XPh})Rh(en)Cl]^+$ (**2**) is in the same range as that obtained with complex $[Cp^*Rh(bpy)Cl]^+$ (**4**).

### 4.3. Reactions with pyruvate

We initially studied the reduction of $NAD^+$, but it is well known that this type of catalyst can also be used for the reduction of other molecules. Previously, the possibility of reducing biomolecules such as pyruvate was reported, using $[(Cp^*)Ir(phen)Cl]^+$ as a catalyst [14]. Therefore, we studied the catalytic reduction of pyruvate using complexes **1**–**9**.

Complexes **1** and **2** reduce pyruvate in the presence of sodium formate, and complete conversion to lactate was achieved. The complex containing the Cp* ring was less active than that containing the extended cyclopentadienyl ring (Fig. 6). Similar to the reduction of $NAD^+$, when using bipyridine (**4**–**6**) and phenanthroline (**7**–**9**) as chelating ligands, the catalytic activity decreases with extended Cp rings. Interestingly, the catalytic activity of compounds **6** and **9** was extremely low, and after 8 h less than 30% conversion was achieved. The complexes containing $Cp^{XPhPh}$ were not able to reduce pyruvate effectively before decomposition, and the reactions cannot be considered as catalytic (Fig. 6).

The low catalytic activity of complexes **1**–**9** for the reduction of pyruvate was expected since both, pyruvate and formate, contain negatively-charged carboxylate groups which can compete with hydride for binding to Rh(III).

### 4.4. Competition for the reduction of $NAD^+$ and pyruvate

Competition experiments were performed using complex $[(Cp^*)Rh(bpy)Cl]^+$ (**4**). For these experiments, 4.5 mol equiv. of $NAD^+$ and pyruvate were reduced using 25 mol equiv. of formate. The experiment showed a clear preference of complex **4** for the reduction of $NAD^+$. $NAD^+$ was reduced completely but at a slight lower rate than when the reaction was performed without pyruvate (Fig. 7), attributable to competitive binding of formate and pyruvate.

Pyruvate was reduced only after the levels of $NAD^+$ became very low. The reduction of pyruvate in the presence of $NAD^+$ was extremely slow compared with the reduction of pyruvate on its own, with 50% reduction of pyruvate to lactate after 2 h 15 min.

### 4.5. Cancer cell growth inhibition

The antiproliferative activity of complexes **1**–**10** in A2780 human ovarian cancer cells was studied (Table 3). $IC_{50}$ values for complexes **1**–**3** and **10** were higher than 100 μM (inactive), while complexes **4**–**9** showed moderate activity, with $IC_{50}$ values between 14 and 65 μM. Higher activities were obtained with the phenanthroline series ($IC_{50}$ (**7**) = 17.8 ± 0.6 μM, (**9**) = 14.68 ± 0.08 μM). Interestingly, in all cases lower $IC_{50}$ values were obtained when using the $Cp^{xPhPh}$ capping ligand, perhaps due to an increase in hydrophobicity and increased accumulation of the metal complex in cells [38,39], or due to the intercalation of the extended aromatic unit between nucleobases of DNA [32,33].

Cell survival with complexes **1**–**10** upon addition of formate at concentrations of 0.5, 1 and 2 mM was also determined (Fig. 8). The complexes show enhanced activity in combination with formate. Formate alone had no effect on cell viability. It seems reasonable to propose that co-administration of the complexes with formate gives rise to catalytic transfer hydrogenation reactions in the A2780 human ovarian cancer cells, although perhaps with few turnovers in view of the variety of nucleophiles in the cell which might terminate the reactions.

In our previous work we have shown that transfer hydrogenation catalysts such as $[(bip)Ru(en)Cl]^+$ or [(*p*-cym)Ru(TfEn)Cl] together with formate can reduce the levels of nicotinamide adenine dinucleotide ($NAD^+$) in cells [12]. $NAD^+$ is an important co-enzyme involved in maintaining the redox balance, the Kerb's cycle and other metabolic pathways such as synthesis of ADP-ribose, ADP-ribose polymers and cyclic ADP-ribose which are crucial for genome stability, DNA repair, and maintenance of calcium homeostasis [40–45]. Changes in the cellular redox status play an important role in cell death. In particular, cancer cells, might be more sensitive to redox variations, since they are under constant oxidative stress due to high production of reactive oxygen species (ROS) [40–45].

Despite the higher catalytic activity towards the reduction of $NAD^+$ of the Rh(III) complexes **1**–**10** compared with the Ru(II) complexes studied previously [15,16], the enhancement in antiproliferative activity of the Rh(III) complexes is not as high as for their Ru(II) analogues [12]. The increase in catalytic activity for the reduction of $NAD^+$ does not correlate with an increase in antiproliferative activity when the drugs are co-administered with sodium formate (Fig. 8b). The inconsistency between the catalytic activity and effects on cells might be due to various factors. The poisoning of the catalyst [46], for example. Ward *et al.* have studied the possibility of synthesizing Ir(III) Noyori-type catalysts capable of reducing $NAD^+$, quinones and ketones [29,47]. In order to reduce poisoning due to sulphur-containing molecules, such as glutathione, the compounds were conjugated to biotin-streptavidine [47]. The artificial metalloenzyme was able to carry out transfer hydrogenation reactions and reduce, to a certain extent, the effect of poisoning due to glutathione [47].

The anticancer activity of the compounds may be due in part not only to the reduction of $NAD^+$ but also other biomolecules. For example, in this work we have demonstrated that complexes **1**–**5** and **7**–**8** can reduce pyruvate, while compounds **6** and **9** cannot. Pyruvate is an essential component of cellular energy pathways (Krebs' cycle) and of special importance in cancer cells. It has been previously observed that cancer cells consume high levels of glucose and release lactate and carbon dioxide (Warburg effect) [48,49]. This behaviour is linked to the malfunctioning of mitochondria. Cancer cells have a high rate of consumption of glucose (glycolysis) due to the need to generate nutrients such as nucleotides and amino acids. However, a high rate of glycolysis, requires high levels of $NAD^+$. Cancer cells regenerate $NAD^+$ at a very fast rate by reducing pyruvate to lactate (Fig. 9) [48,49].

In the presence of the Rh(III) catalysts **1**–**5** and **7**–**8**, the pool of pyruvate in cells may be reduced due to conversion to lactate. As a consequence, the regeneration of $NAD^+$ and the anaerobic glycolysis in cancer cells will be disrupted. The reduction of pyruvate, in combination with the reduction of $NAD^+$ will affect not only the redox regulatory

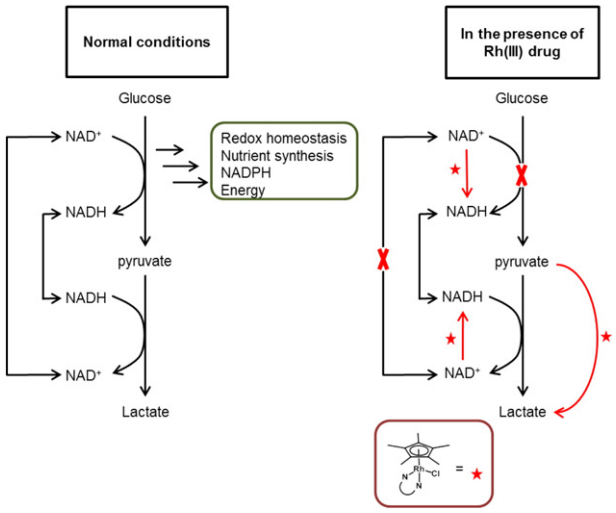


**Fig. 9.** Anaerobic glycolysis and role of pyruvate in cancer cells under normal conditions (left) and possible effects due to the presence of Rh(III) complexes co-administered with sodium formate.

system of the cell, but also the generation of ATP (energy) and formation of various nutrients necessary for cell growth and reproduction.

## 5. Conclusions

During the last decade, there has been increasing interest in developing metal-based catalysts which are effective in cells. Such technology might be useful in areas such as protein labelling, imaging, and for the treatment of diseases. For example, Chen and Meggers have shown that metal compounds such as $Pd(dba)_2$ or $[CpRu(QA)(\eta^3\text{-allyl})]PF_6$ (QA = 2-quinolinecarboxylate) can be used to remove protector groups from N-protected anticancer drugs [50,51]. Cowan *et al.* have shown that Cu(II)/Ni(II)-ATCUN compounds can decompose RNA in hepatitis or HIV [52,53]. Also organo-ruthenium compounds can oxidise glutathione catalytically [54].

In the current work, we have studied the possibility that the Rh(III) complexes $[(Cp^x)Rh(N,N')Cl]$ may be more active catalysts than their Ru(II) arene analogues. Four series of compounds which can reduce $NAD^+$ to NADH using formate as a hydride source, have been investigated under biologically-relevant conditions (aqueous solution, pH = 7.2, 310 K). The catalytic activity decreased in the order of *N*,*N*-chelated ligand bpy > phen > en with Cp* as the $\eta^5$-donor. However, while the ethylenediamine-containing compounds (**1–3**) became more active with extension to the $Cp^X$ ring, we observed a decrease in catalytic activity for *N*,*N*-chelated phenanthroline- (**7–9**) and bipyridine– (**4–6**) compounds, perhaps due to an increase in steric hindrance. The complex $[Cp^*Rh(bpy)Cl]^+$ (**4**) showed the highest catalytic activity towards the reduction of $NAD^+$, with a TOF of 37.4 ± 2 $h^{-1}$.

The catalytic activity of complexes $[Cp^xRh(en)Cl]^+$ (**1–3**) (7.50, 19.65 and 24.19 $h^{-1}$, respectively) is up to two orders of magnitude higher than for their Ru(II) analogues (TOF [(hmb)Ru(en)Cl] + = 0.85 $h^{-1}$). Interestingly, Noyori type Rh(III) compounds such as **10** with a turnover frequency of 4.12 $h^{-1}$, display no marked improvement compared to the Ru(II) arene analogues (c.f. 6.62 $h^{-1}$ for [(bn)Ru(TfEn)Cl]).

Mechanistic studies on these Rh(III) complexes were carried out in order to investigate the catalytic cycle. Fast hydrolysis of the chlorido complexes **1–10** was observed by $^1H$ NMR (<10 min at 310 K). Compounds **1–3** and **10** gave quantitative conversion to aqua adducts, while complexes **4–9** (at millimolar concentrations) reached equilibrium with a 30–60% of the aqua species present. The $pK_a^*$ values determined for the aqua adducts of ca. 8–10 indicate that the Rh(III) complexes are likely to be present in their aqua forms around pH 7 rather than forming less reactive hydroxido species. Complexes **1** and **10** showed a dependence of the reaction rate on formate concentration, but not on $NAD^+$ concentration. No reaction between complexes **1–4** and 1,4-NADH was detected after 10 h. Optimum pH* for the reaction with complex **1** was 7.3 ± 0.1, close to physiological pH. These results indicate that these Rh(III) $Cp^x$ compounds exhibit similar behaviour to their Ru(II) arene analogues.

The maximum turnover frequencies of Rh(III) complexes **1** and **10** of 41.5 and 37.2 $h^{-1}$, respectively, at high concentrations of formate are significant improvements in catalytic activity compared to the Ru(II) analogues (6.9 $h^{-1}$), even for complex $[(Cp^*)Rh(TfEn)Cl]$ **(10)**. This improvement in the maximum turnover frequency might be expected to translate in significant enhancements in antiproliferative activity towards cancer cells when the complexes are used in combination with high concentrations of formate.

We also demonstrated that some Rh(III) complexes, notably **1–5**, **7** and **8**, can catalyse the reduction of pyruvate to lactate using formate as the hydride donor. Such reactions might occur in cells. However complexes **6** and **9** with very low TOFs are not effective catalysts. The transfer hydrogenation reactions were shown to be greatly affected by the chelating ligand and the capping $Cp^x$ ring. The catalytic activity of ethylenediamine compounds (**1–3**) increases for extended $Cp^x$ rings, while the bipyridine and phenanthroline compounds (**4–9**) show the opposite trend. Studies of competition reactions between $NAD^+$ and pyruvate for reduction by formate catalysed by complex **4** suggested a clear preference for the reduction of $NAD^+$, although, some lactate was still formed.

The antiproliferative activity of the Rh(III) complexes towards A2780 human ovarian cancer cells increased by up to 50% (for complex **3**) when administered in combination with formate. However, the improvement in the activity of these Rh(III) complexes induced by formate is much lower than in the case of Ru(II) complexes. It is possible that Rh(III) centres, being more reactive than Ru(II), are more easily poisoned in the complicated mixture of biomolecules present in culture media and in cells.

## Abbreviations

| | |
|---|---|
| $Cp^*$ | pentamethylcyclopenadienyl |
| $Cp^{xPh}$ | 1-phenyl-2,3,4,5-tetramethylcyclopentadienyl |
| $Cp^{xPhPh}$ | 1-biphenyl-2,3,4,5-tetramethylcyclopentadienyl |
| *p*-cym | *p*-cymene |
| bn | benzene |
| hmb | hexamethylbenzene |
| bip | biphenyl |
| bpy | 2,2′-bipyridine; phen, phenanthroline |
| TOF | turnover frequency |
| TON | turnover number |
| $NAD^+$ | nicotinamide adenine dinucleotide |
| NADH | reduced nicotinamide adenine dinucleotide |
| en | ethylenediamine |
| TfEn | N-(2-aminoethyl)-4-(trifluoromethyl)benzenesulfonamide |
| TsEn | N-(2-aminoethyl)-4-toluene sulfonamide |
| TsDPEN | (N-[(R,2R)-2-amino-1,2-diphenylethyl]-4-toluene sulfonamide) |

## Acknowledgements

We thank the ERC (grant no. 247450) EPSRC (grant no. EP/F042159/1), ERDF/AWM (Science City), and Mr. Josep A. S. (scholarship for J.J.S.B) for the support, Dr. Ivan Prokes for the advice and help with NMR, and members of EU COST Action CM1105 for their stimulating discussions.

## References

[1] S. Ogo, T. Matsumoto, A. Robertson, The development of aqueous transfer hydrogenation catalysts, Dalton Trans. 40 (2011) 10304–10310.
[2] X. Wu, C. Wang, J. Xiao, Asymmetric transfer hydrogenation in water with platinum group metal catalysts, Platin. Met. Rev. 54 (2010) 3–19.
[3] S. Gladiali, E. Alberico, Asymmetric transfer hydrogenation: chiral ligands and applications, Chem. Soc. Rev. 35 (2006) 226–236.
[4] P. Brandt, P.G. Andersson, J. Backvall, J.S.M. Samec, Mechanistic aspects of transition metal-catalyzed hydrogen transfer reactions, Chem. Soc. Rev. 35 (2006) 237–248.
[5] T.R. Ward, Artificial metalloenzymes based on the biotin–avidin technology: enantioselective catalysis and beyond, Acc. Chem. Res. 44 (2011) 47–57.
[6] J. Wu, F. Wang, Y. Ma, X. Cui, L. Cun, J. Zhu, J. Deng, B. Yu, Asymmetric transfer hydrogenation of imines and iminiums catalyzed by a water-soluble catalyst in water, Chem. Commun. 1766-1768 (2006).
[7] D.S. Matharu, D.J. Morris, G.J. Clarkson, M. Wills, An outstanding catalyst for asymmetric transfer hydrogenation in aqueous solution and formic acid/triethylamine, Chem. Commun. (2006) 3232–3234.
[8] T. Völker, E. Meggers, Transition-metal-mediated uncaging in living human cells—an emerging alternative to photolabile protecting groups, Curr. Opin. Chem. Biol. 25 (2015) 48–54.
[9] J.J. Soldevila-Barreda, P.J. Sadler, Approaches to the design of catalytic metallodrugs, Curr. Opin. Chem. Biol. 25 (2015) 172–183.
[10] P.K. Sasmal, C.N. Streu, E. Meggers, Metal complex catalysis in living biological systems, Chem. Commun. 49 (2013) 1581–1587.
[11] A.L. Noffke, A. Habtemariam, A.M. Pizarro, P.J. Sadler, Designing organometallic compounds for catalysis and therapy, Chem. Commun. 48 (2012) 5219–5246.
[12] J.J. Soldevila-Barreda, I. Romero-Canelón, A. Habtemariam, P.J. Sadler, Transfer hydrogenation catalysis in cells as a new approach to anticancer drug design, Nat. Commun. 6 (2015) 6582 (1–9).
[13] Z. Liu, I. Romero-Canelón, B. Qamar, J.M. Hearn, A. Habtemariam, N.P.E. Barry, A.M. Pizarro, G.J. Clarkson, P.J. Sadler, The potent oxidant anticancer activity of organoiridium catalysts, Angew. Chem. Int. Ed. 53 (2014) 3941–3946.

[14] S. Betanzos-Lara, Z. Liu, A. Habtemariam, A.M. Pizarro, B. Qamar, P.J. Sadler, Organometallic ruthenium and iridium transfer-hydrogenation catalysts using coenzyme NADH as a cofactor, Angew. Chem. Int. Ed. 51 (2012) 3897–3900.

[15] J.J. Soldevila-Barreda, P.C.A. Bruijnincx, A. Habtemariam, G.J. Clarkson, R.J. Deeth, P.J. Sadler, Improved catalytic activity of ruthenium–arene complexes in the reduction of NAD+, Organometallics 31 (2012) 5958–5967.

[16] Y.K. Yan, M. Melchart, A. Habtemariam, A.F. Peacock, P.J. Sadler, Catalysis of regioselective reduction of $NAD^+$ by ruthenium(II) arene complexes under biologically relevant conditions, J. Biol. Inorg. Chem. 11 (2006) 483–488.

[17] A.J. Millett, A. Habtemariam, I. Romero-Canelón, G.J. Clarkson, P.J. Sadler, Contrasting anticancer activity of half-sandwich iridium(III) complexes bearing functionally diverse 2-phenylpyridine ligands, Organometallics 34 (2015) 2683–2694.

[18] Z. Liu, A. Habtemariam, A.M. Pizarro, S.A. Fletcher, A. Kisova, O. Vrana, L. Salassa, P.C.A. Bruijnincx, G.J. Clarkson, V. Brabec, et al., Organometallic half-sandwich iridium anticancer complexes, J. Med. Chem. 54 (2011) 3011–3026.

[19] M. Björgvinsson, S. Halldorsson, I. Arnason, J. Magull, D. Fenske, Preparation and characterization of $(C_5Me_4Ph)TiCl_3$, the oxochloride complexes $[(C_5Me_4Ph)TiCl_2]_2(\mu\text{-}O)$ and $[(C_5Me_4Ph)TiCl(\mu\text{-}O)]_3$ and the oxo-complex$[(C_5Me_4Ph)Ti]_4(\mu\text{-}O)_6$. The X-ray crystal structures of $[(C_5Me_4Ph)TiCl_2]_2(\mu\text{-}O)$ and $[(C_5Me_4Ph)Ti]_4(\mu\text{-}O)_6$, J. Organomet. Chem. 544 (1997) 207–215.

[20] G. Garcia, G. Sanchez, I. Romero, I. Solano, M.D. Santana, G. Lopez, Reactivity of $[\{\eta^5\text{-}C_5Me_5RhCl(\mu\text{-}Cl)\}_2]$ towards some potentially bidentate ligands, J. Organomet. Chem. 408 (1991) 241–246.

[21] P. Skehan, R. Storeng, D. Scudiero, A. Monks, J. McMahon, D. Vistica, J.T. Warren, H. Bokesch, S. Kenney, M.R. Boyd, New colorimetric cytotoxicity assay for anticancer-drug screening, J. Natl. Cancer Inst. 82 (1990) 1107–1112.

[22] T. Quinto, V. Köhler, T.R. Ward, Recent trends in biomimetic NADH regeneration, Top. Catal. 57 (2014) 321–331.

[23] H. Wu, C. Tian, X. Song, C. Liu, D. Yang, Z. Jiang, Methods for the regeneration on NAD coenzymes, Green Chem. 15 (2013) 1773–1789.

[24] V. Uppada, S. Bhaduri, S.B. Noronha, Cofactor regeneration — an important aspect of biocatalysis, Curr. Sci. 106 (2014) 946–957.

[25] P. Haquette, B. Talbi, L. Barilleau, N. Madern, C. Fosse, M. Salmain, Chemically engineered papain as artificial formate dehydrogenase for NAD(P)H regeneration, Org. Biomol. Chem. 9 (2011) 5720–5727.

[26] J. Canivet, G. Süss-Fink, P. Štěpnička, Water-soluble phenanthroline complexes of rhodium, iridium and ruthenium for the regeneration of NADH in the enzymatic reduction of ketones, Eur. J. Inorg. Chem. (2007) 4736–4742.

[27] R. Ruppert, S. Herrmann, E. Steckhan, Very efficient reduction of NAD $(P)^+$ with formate catalysed by cationic rhodium complexes, Chem. Commun. (1988) 1150–1151.

[28] J. Lutz, F. Hollmann, T.V. Ho, A. Schnyder, R.H. Fish, A. Schmid, Bioorganometallic chemistry: biocatalytic oxidation reactions with biomimetic NAD+/NADH cofactors and $[Cp^*Rh(bpy)H]^+$ for selective organic synthesis, J. Organomet. Chem. 689 (2004) 4783–4790.

[29] T. Quinto, D. Haussinger, V. Kohler, T.R. Ward, Artificial metalloenzymes for the diastereoselective reduction of $NAD^+$ to $NAD^2H$, Org. Biomol. Chem. 13 (2015) 357–360.

[30] M. de Torres, J. Dimroth, I.W.C.E. Arends, J. Keilitz, F. Hollmann, Towards recyclable NAD(P)H regeneration catalysts, Molecules 17 (2012) 9835–9841.

[31] X. Wu, J. Liu, X. Li, A. Zanotti-Gerosa, F. Hancock, D. Vinci, J. Ruan, J. Xiao, On water and in air: fast and highly chemoselective transfer hydrogenation of aldehydes with iridium catalysts, Angew. Chem. Int. Ed. 45 (2006) 6718–6722.

[32] J.C. García-Ramos, R. Galindo-Murillo, F. Cortés-Guzmán, L. Ruiz-Azuara, Metal-based drug–DNA interactions, J. Mex. Chem. Soc. 57 (2013) 245–259.

[33] H.K. Liu, P.J. Sadler, Metal complexes as DNA intercalators, Acc. Chem. Res. 44 (2011) 349–359.

[34] J. Václavík, P. Kačer, M. Kuzma, L. Červený, Opportunities offered by chiral $\eta^6$-arene/N-arylsulfonyl-diamine-$Ru^{II}$ catalysts in the asymmetric transfer hydrogenation of ketones and imines, Molecules 16 (2011) 5460–5495.

[35] A. Robertson, T. Matsumoto, S. Ogo, The development of aqueous transfer hydrogenation catalysts, Dalton Trans. 40 (2011) 10304–10310.

[36] H.C. Lo, C. Leiva, O. Buriez, J.B. Kerr, M.M. Olmstead, R.H. Fish, Regioselective reduction of $NAD^+$ models, 1-benzylnicotinamde triflate and beta-nicotinamide ribose-5′-methyl phosphate, with in situ generated $[Cp^*Rh(Bpy)H]^+$: structure–activity relationships, kinetics, and mechanist, Inorg. Chem. 40 (2001) 6705–6716.

[37] Z. Liu, R.J. Deeth, J.S. Butler, A. Habtemariam, M.E. Newton, P.J. Sadler, Reduction of Quinones by NADH catalyzed by organoiridium complexes, Angew. Chem. Int. Ed. 52 (2013) 4194–4197.

[38] M. Hanif, A.A. Nazarov, C.G. Hartinger, W. Kandioller, M.A. Jakupec, V.B. Arion, P.J. Dyson, B.K. Keppler, Osmium(ii)-versus ruthenium(ii)-arene carbohydrate-based anticancer compounds: similarities and differences, Dalton Trans. 39 (2010) 7345–7352.

[39] S.H. van Rijt, A.F.A. Peacock, R.D.L. Johnstone, S. Parsons, P.J. Sadler, Organometallic osmium(II) arene anticancer complexes containing picolinate derivatives, Inorg. Chem. 48 (2009) 1753–1762.

[40] R.H. Houtkooper, J. Auwerx, Exploring the therapeutic space around $NAD^+$, J. Cell Biol. 199 (2012) 205–209.

[41] A. Chiarugi, C. Dölle, R. Felici, M. Ziegler, The NAD metabolome — a key determinant of cancer cell biology, Nat. Rev. 12 (2012) 741–752.

[42] R.H. Houtkooper, C. Canto, R.J. Wanders, J. Auwerx, The secret life of $NAD^+$: an old metabolite controlling new metabolic signaling pathways, Endocr. Rev. 31 (2010) 194–223.

[43] W. Ying, $NAD^+$/NADH and $NADP^+$/NADPH in cellular functions and cell death: regulation and biological consequences, Antioxid. Redox Signal. 10 (2008) 179–206.

[44] P. Belenky, K.L. Bogan, C. Brenner, $NAD^+$ metabolism in health and disease, Trends Biochem. Sci. 32 (2007) 12–19.

[45] W. Ying, NAD+ and NADH in cellular functions and cell death, Front. Biosci. 1 (2006) 3129–3148.

[46] R.H. Crabtree, Deactivation in homogeneous transition metal catalysis: causes, avoidance, and cure, Chem. Rev. 115 (2015) 127–150.

[47] Y.M. Wilson, M. Dürrenberger, E.S. Nogueira, T.R. Ward, Neutralizing the detrimental effect of glutathione on precious metal catalysts, J. Am. Chem. Soc. 136 (2014) 8928–8932.

[48] M.G. Vander Heiden, L.C. Cantley, C.B. Thompson, Understanding the Warburg effect: the metabolic requirements of cell proliferation, Science 324 (2009) 1029–1033.

[49] F. Hirschhaeuser, U.G. Sattler, W. Mueller-Klieser, Lactate: a metabolic key player in cancer, Cancer Res. 71 (2011) 6921–6925.

[50] J. Li, J. Yu, J. Zhao, J. Wang, S. Zheng, S. Lin, L. Chen, M. Yang, S. Jia, X. Zhang, et al., Palladium-triggered deprotection chemistry for protein activation in living cells, Nat. Chem. 6 (2014) 352–361.

[51] T. Völker, F. Dempwolff, P.L. Graumann, E. Meggers, Progress towards ioorthogonal catalysis with organometallic compounds, Angew. Chem. Int. Ed. 53 (2014) 10536–10540.

[52] S.S. Bradford, M.J. Ross, I. Fidai, J.A. Cowan, Insight into the recognition, binding, and reactivity of catalytic metallodrugs targeting stem loop IIb of hepatitis C IRES RNA, Chem. Med. Chem. 9 (2014) 1275–1285.

[53] J.C. Joyner, K.D. Keuper, J.A. Cowan, Kinetics and mechanisms of oxidative cleavage of HIV RRE RNA by rev-coupled transition metal chelates, Chem. Sci. 4 (2013) 1707–1718.

[54] S.J. Dougan, A. Habtemariam, S.E. McHale, S. Parsons, P.J. Sadler, Catalytic organometallic anticancer complexes, Proc. Natl. Acad. Sci. U. S. A. 105 (2008) 11628–11633.

[55] F. Wang, J. Xu, A. Habtemariam, P.J. Sadler, Competition between glutathione and guanine for a ruthenium(II) arene anticancer complex: detection of a sulfenato intermediate, J. Am. Chem. Soc. 127 (2005) 17734–17743.

[56] F. Wang, A. Habtemariam, E.P.L. van der Geer, R. Fernández, M. Melchart, R.J. Deeth, R. Aird, S. Guichard, F.P. Fabbiani, P. Lozano-Casal, et al., Controlling ligand substitution reactions of organometallic complexes: tuning cancer cell cytotoxicity, Proc. Natl. Acad. Sci. U. S. A. 102 (2005) 18269–18274.